

**NAVAL POSTGRADUATE SCHOOL**  
**Monterey, California**



**THESIS**

**ENERGETIC ELECTRON GENERATION BY FORWARD  
STIMULATED RAMAN SCATTERING USING 0.35 AND  
0.53 MICRON LASER LIGHT IN A PLASMA**

by

Michael A. Ortelli

June 2001

Thesis Advisor:  
Second Reader:

William L. Kruer  
William B. Colson

**Approved for public release; distribution is unlimited**

**20011108 167**

|   |   |  |  |  |
|---|---|--|--|--|
| <b>REPORT DOCUMENTATION PAGE</b>  |   |  | Form Approved OMB No. 0704-0188                            |  |
| Public reporting burden for this collection of information is estimated to average 1 hour per response, including the time for reviewing instruction, searching existing data sources, gathering and maintaining the data needed, and completing and reviewing the collection of information. Send comments regarding this burden estimate or any other aspect of this collection of information, including suggestions for reducing this burden, to Washington headquarters Services, Directorate for Information Operations and Reports, 1215 Jefferson Davis Highway, Suite 1204, Arlington, VA 22202-4302, and to the Office of Management and Budget, Paperwork Reduction Project (0704-0188) Washington DC 20503.   |   |  |  |  |
| <b>1. AGENCY USE ONLY (Leave blank)</b>   |   | <b>2. REPORT DATE</b><br>June 2001                             | <b>3. REPORT TYPE AND DATES COVERED</b><br>Master's Thesis |  |
| <b>4. TITLE AND SUBTITLE:</b><br>ENERGETIC ELECTRON GENERATION BY FORWARD STIMULATED RAMAN SCATTERING USING 0.35 AND 0.53 MICRON LASER LIGHT IN A PLASMA  |   |  | <b>5. FUNDING NUMBERS</b>                                  |  |
| <b>6. AUTHOR(S)</b> Ortelli, Michael A.   |   |  |  |  |
| <b>7. PERFORMING ORGANIZATION NAME(S) AND ADDRESS(ES)</b><br>Naval Postgraduate School, Monterey, CA 93943-5000   |   |  | <b>8. PERFORMING ORGANIZATION REPORT NUMBER</b>            |  |
| <b>9. SPONSORING / MONITORING AGENCY NAME(S) AND ADDRESS(ES)</b> N/A  |   |  | <b>10. SPONSORING / MONITORING AGENCY REPORT NUMBER</b>    |  |
| <b>11. SUPPLEMENTARY NOTES</b> The views expressed in this thesis are those of the author and do not reflect the official policy or position of the Department of Defense or the U.S. Government.   |   |  |  |  |
| <b>12a. DISTRIBUTION / AVAILABILITY STATEMENT</b><br>Approved for public release: distribution is unlimited   |   |  | <b>12b. DISTRIBUTION CODE</b>                              |  |
| <b>13. ABSTRACT (maximum 200 words)</b><br>This research investigates the use of high-powered lasers to produce 50-100 keV x-ray sources for applications for programs such as Stockpile Stewardship and nuclear weapons effects testing (NWET). To produce these x-ray sources requires irradiating targets with intense laser light to efficiently generate high-energy electrons. Stimulated Raman scattering (SRS) of intense laser light produces electron plasma waves, which in turn generate high-energy electrons. To make a high-energy x-ray source, the maximization of this laser-driven instability is desired. Using computer simulations, we show that SRS can be driven by using a combination of frequency-tripled and a "seed" beam of frequency doubled Neodymium laser light in a plasma of the appropriate density. Electron plasma waves with a high phase velocity are produced, which trap electrons and accelerate them to high energy. These energetic electrons will in turn generate high energy x-rays via collisions with nearby dense material. By adjusting the angle between the 0.35 $\mu\text{m}$ and 0.53 $\mu\text{m}$ laser beams, the characteristic temperature of the heated electrons (and the x-rays) can be varied. We show one and two-dimensional simulations and illustrate the important role that laser-driven ion fluctuations play. |   |  |  |  |
| <b>14. SUBJECT TERMS</b><br>Laser-plasma interactions, stimulated Raman scattering, plasma instabilities  |   |  | <b>15. NUMBER OF PAGES</b><br>58                           |  |
|   |   |  | <b>16. PRICE CODE</b>                                      |  |
| <b>17. SECURITY CLASSIFICATION OF REPORT</b><br>Unclassified  | <b>18. SECURITY CLASSIFICATION OF THIS PAGE</b><br>Unclassified | <b>19. SECURITY CLASSIFICATION OF ABSTRACT</b><br>Unclassified | <b>20. LIMITATION OF ABSTRACT</b><br>UL                    |  |

THIS PAGE INTENTIONALLY LEFT BLANK

Approved for public release; distribution is unlimited

**ENERGETIC ELECTRON GENERATION BY FORWARD STIMULATED  
RAMAN SCATTERING USING 0.35 AND 0.53 MICRON LASER LIGHT IN A  
PLASMA**

Michael A. Ortelli  
Major, United States Army  
Engineering Physics, United States Military Academy, 1990

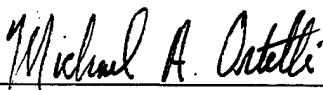
Submitted in partial fulfillment of the  
requirements for the degree of

**MASTER OF SCIENCE IN APPLIED PHYSICS**

from the

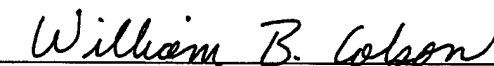
**NAVAL POSTGRADUATE SCHOOL  
June 2001**

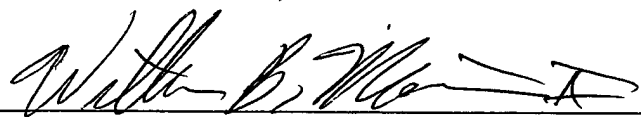
Author:

  
Michael A. Ortelli

Approved by:

  
William L. Kruer, Thesis Advisor

  
William B. Colson, Second Reader

  
William Maier II, Chairman  
Department of Physics

THIS PAGE INTENTIONALLY LEFT BLANK

## ABSTRACT

This research investigates the use of high-powered lasers to produce 50-100 keV x-ray sources for applications for programs such as Stockpile Stewardship and nuclear weapons effects testing (NWET). This requires irradiating targets with intense laser light to efficiently generate high-energy electrons. Stimulated Raman scattering (SRS) of intense laser light produces electron plasma waves, which in turn generate high-energy electrons. To make a high-energy x-ray source, the maximization of this laser-driven instability is desired. Using computer simulations, we show that forward SRS can be driven by using a combination of frequency-tripled and a "seed" beam of frequency doubled Neodymium laser light in a plasma of the appropriate density. Electron plasma waves with a high phase velocity are produced, which trap electrons and accelerate them to high energy. These energetic electrons will in turn generate high energy x-rays via collisions with nearby dense material. By adjusting the angle between the 0.35  $\mu\text{m}$  and 0.53  $\mu\text{m}$  laser beams, the characteristic temperature of the heated electrons (and the x-rays) have been varied. We show one and two-dimensional simulations and illustrate the important role that laser-driven ion fluctuations play.

THIS PAGE INTENTIONALLY LEFT BLANK

## TABLE OF CONTENTS

|  |           |
|--|-----------|
| <b>I. INTRODUCTION.....</b>  | <b>1</b>  |
| A. MOTIVATION AND APPLICATION .....  | 1         |
| B. DESCRIPTION OF RESEARCH.....  | 2         |
| <b>II. THEORY.....</b>   | <b>5</b>  |
| A. LASER-PLASMA INTERACTIONS AND INSTABILITIES .....   | 5         |
| B. COMPUTER SIMULATIONS AND MODELING PLASMA<br>INSTABILITIES.....                                      | 17        |
| <b>III. RESULTS AND ANALYSIS.....</b>  | <b>21</b> |
| A. SIMULATIONS OF $3\omega$ (BACKSCATTER) AND $3\omega$ AND $2\omega$<br>(SEEDED FORWARD SCATTER)..... | 21        |
| B. DATA ANALYSIS .....   | 32        |
| <b>IV. CONCLUSIONS.....</b>  | <b>35</b> |
| LIST OF REFERENCES .....   | 37        |
| INITIAL DISTRIBUTION.....  | 39        |

THIS PAGE INTENTIONALLY LEFT BLANK

## LIST OF FIGURES

|  |    |
|--|----|
| Figure 1 Stimulated Raman scattering in backward and forward direction.....              | 3  |
| Figure 2 Plasma instability feedback loop for Raman backscatter .....                    | 7  |
| Figure 3 Plasma instability feedback loop for forward scatter .....                      | 12 |
| Figure 4 Electric field in the z-direction (incident and scattered wave) .....           | 23 |
| Figure 5 Electron plasma wave electric field in the x-direction .....                    | 23 |
| Figure 6 Momentum of electrons in plasma wave in the x-direction .....                   | 23 |
| Figure 7 Energy plot for SRS backscatter.....  | 24 |
| Figure 8 Electron distribution plot for SRS backscatter .....                            | 24 |
| Figure 9 Electric field in the z-direction (incident and seed beam) .....                | 26 |
| Figure 10 Electron plasma wave electric field in the x-direction .....                   | 26 |
| Figure 11 Momentum of electrons in plasma wave in the x-direction .....                  | 26 |
| Figure 12 Energy plot for seeded forward SRS .....                                       | 27 |
| Figure 13 Electron distribution plot for seeded forward SRS.....                         | 27 |
| Figure 14 Energy plot for seeded forward SRS, 2 beams at 30 degrees.....                 | 29 |
| Figure 15 Electron distribution plot for seeded forward SRS, 2 beams at 30 degrees ..... | 29 |
| Figure 16 Ion wave for forward scatter with seed beam.....                               | 30 |
| Figure 17 Energy plot for seeded forward SRS with moving ions .....                      | 31 |
| Figure 18 Electron distribution plot for seeded forward SRS with moving ions.....        | 31 |
| Figure 19 Calculated and Simulated value plot for forward SRS with seed beam.....        | 32 |
| Figure 20 Resonance absorption plot for varying density .....                            | 34 |

THIS PAGE INTENTIONALLY LEFT BLANK

## LIST OF SYMBOLS AND ACRONYMS

|               |   |
|---------------|---|
| $\omega_o$    | incident laser frequency (if two lasers, subscripted 1 and 2)   |
| $\omega_{pe}$ | electron plasma frequency   |
| $\omega_{ek}$ | Bohm-Gross corrected electron plasma frequency  |
| $k_o$         | wave number of incident laser light ( $2\pi/\lambda$ )  |
| $k_{sc}$      | wave number of scattered light wave   |
| $k_{plasma}$  | wave number of electron plasma wave   |
| $k_B$         | Boltzman's constant   |
| $c$           | speed of light in a vacuum  |
| $\lambda$     | wavelength (in $\mu m$ )  |
| $I$           | laser intensity ( $W/cm^2$ )  |
| $e$           | electron charge   |
| $m$           | electron mass   |
| $E$           | Electric field ( $E_x$ will denote the electric field of the plasma wave, $E_z$ for the electric field of the laser light wave)                       |
| $v_{os}$      | oscillation velocity of electron in an electric field. Defined as $eE/m\omega_o$ .  |
| $a$           | simulation variable for the electron oscillation velocity divided by the speed of light   |
| $v_{th}$      | electron thermal velocity   |
| $T$           | temperature (in keV) of electron ( $T_e$ ) or ions ( $T_i$ ). $T_{hot}$ denotes the temperature of the hot electron tail of the electron distribution |
| $v_{phase}$   | phase velocity of electron plasma wave  |
| $n$           | plasma density  |
| $n_{cr}$      | critical density. The density at which $k$ of the light wave becomes imaginary, light no longer propagates through plasma                             |
| SRS           | stimulated Raman scattering   |
| SBS           | stimulated Brillouin scattering   |

THIS PAGE INTENTIONALLY LEFT BLANK

## ACKNOWLEDGMENTS

- Dr. William L. Kruer, for motivating my interest in the field of plasma physics and computer simulation, and supporting me in this research. His invaluable expertise and enthusiasm made for a perfect mentor. I am forever grateful for his assistance.
- The plasma simulation capability at NPS and the collaborations with UCLA were made possible by support from the Defense Threat Reduction Agency under NPS contract RPH4J.
- I gratefully acknowledge collaborations with Prof. Warren Mori, Dr. Chuang Ren and Dr. Frank Tsung of UCLA and with Dr. Dan Gordon of NRL for assistance in analysis and troubleshooting of plasma simulations.
- I also extend thanks to Bob Kirkwood of LLNL and Prof. Olson of NPS for their assistance in preliminary experimental data analysis of SRS.

THIS PAGE INTENTIONALLY LEFT BLANK

## I. INTRODUCTION

### A. MOTIVATION AND APPLICATION

The study of laser matter interaction for the goal of producing inertial confinement fusion (ICF) has been ongoing for many years [Ref. 1]. As the Lawrence Livermore National Laboratory (LLNL) looks forward to the completion of the National Ignition Facility (NIF), many interesting questions have been posed about other potential applications of NIF in addition to fusion research.

One interesting application is the production of energetic electrons to produce hard x-rays, on the order of 50 keV and higher [Ref. 2]. A high flux of these high-energy x-rays can be useful in certain applications in the Nuclear Weapons Effects Testing (NWET) and Stockpile Stewardship programs. Previously, with the Livermore Shiva laser (now decommissioned), the use of  $1.06\text{ }\mu\text{m}$  light was found to produce strong plasma waves efficiently, which could accelerate electrons in the plasma, and cause a high-energy tail to develop in the electron distribution of the plasma. It was found that the energetic electrons that were produced would be detrimental to the ICF program, as the electrons would pre-heat the fuel capsule, and prevent the large compression required for fusion. To reduce the growth of these plasma waves to near the instability threshold, the  $1.06\text{ }\mu\text{m}$  laser was frequency-tripled so that this incident laser light has a wavelength of  $0.351\text{ }\mu\text{m}$ . As expected, this instability generation was then much reduced; since the instability growth is a function of intensity  $I$  times the square of the wavelength of the incident laser light [Ref. 1]. The reduction of this instability growth was most recently demonstrated in recent laser-plasma interaction experiments [Ref. 3] conducted by LLNL

experimentalists at the OMEGA facility of the University of Rochester. In these experiments, which used  $0.35\mu\text{m}$  light alone with high density targets, only about 0.01% Raman backscatter occurred, meaning that only a very small amount of absorption of the laser went into producing hot electrons.

However, for other applications of NIF, one may want to maximize high-energy electron generation. NIF could then be used as a high-energy x-ray source for nuclear weapons effects testing. This motivates an exploration of a technique to enhance high-energy electron production; i.e., by "seeding" the instability generation when it is desired.

## **B. DESCRIPTION OF RESEARCH**

The goal of this thesis is to demonstrate the feasibility of using a "seed" beam at  $.53\mu\text{m}$  in combination with a  $.35\mu\text{m}$  beam, to generate, through forward SRS, high phase velocity electron plasma waves. These waves in turn accelerate electrons, which subsequently produce hard x-rays from electron-ion collisions.

The thesis begins with an introduction into the basic theories of plasma instabilities and the specific cases of interest. Then some of the ideas behind computer simulation and how the theory is incorporated into simulations are discussed. In the results and analysis section, computer simulations are used to show that by "seeding"  $.35\mu\text{m}$  light with  $.53\mu\text{m}$  light in a plasma of appropriate density, high-energy electrons can be produced to give the desired hard x-ray flux. Further, by varying the angle between the two beams, the temperature of the electrons and thus the energy of the x-ray flux can be controlled. Use of this technique would only require that some NIF beams be frequency-doubled rather than tripled.

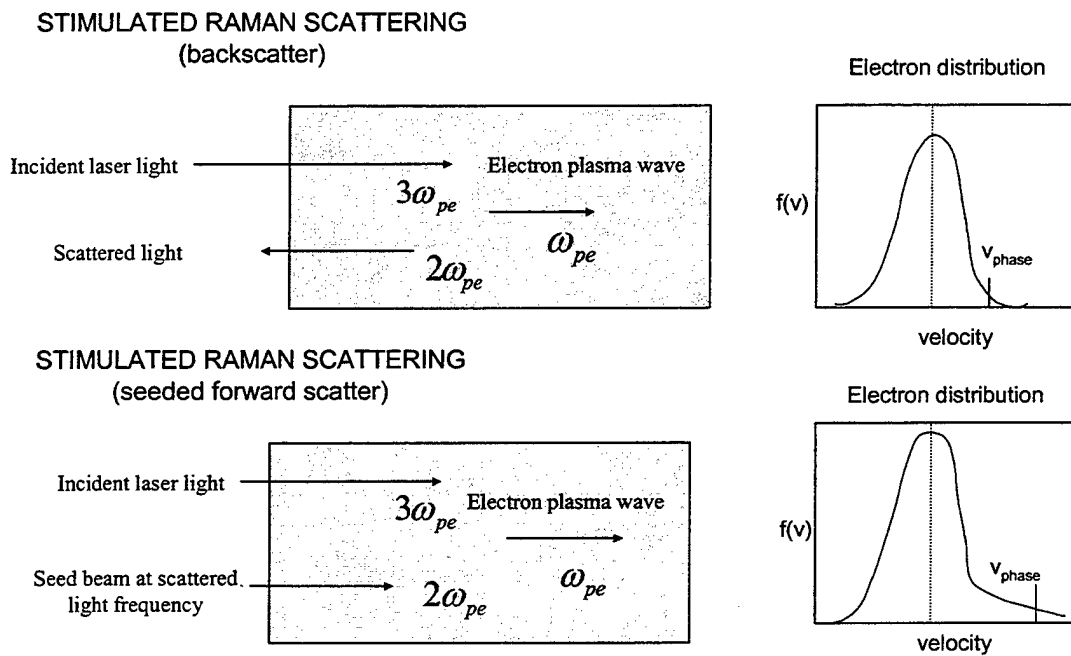


**Figure 1. Stimulated Raman Scattering in Forward and Backward Direction.**

**The distribution plots show the relative location of the phase velocity of the electron plasma wave.**

THIS PAGE INTENTIONALLY LEFT BLANK

## II. THEORY

### A. LASER-MATTER INTERACTION AND INSTABILITIES

#### 1. Introduction

Laser-plasma coupling has been intensely studied for many years for the interesting non-linear processes that take place and their potential application towards achieving inertial fusion and other applications [Ref. 1]. Many nonlinear optical processes appear, including stimulated Raman scattering (SRS) from electron plasma waves, stimulated Brillouin scattering (SBS) from ion sound waves and laser beam self-focusing and filamentation. The magnitude of these processes depends upon laser intensity and plasma densities and produce effects such as changes in the efficiency and location of the absorption and generation of very energetic electrons. Depending on the application, one wishes to either minimize or maximize various non-linear processes.

For the purpose of this thesis, we wish to investigate the possibility of the SRS in the forward scattered direction. It is necessary to describe in some detail the process by which instabilities such as SRS are produced and the differences between forward scatter and backscatter, as it will better explain the motivations for the simulations that have been conducted.

Different instabilities can develop when a strongly driven electromagnetic wave (specifically a laser at  $\sim 10^{15}$  W/cm<sup>2</sup>) interacts with a dense plasma. [Ref 1.] In the case where dc magnetic fields are negligible, we can simply describe these instabilities as resonant mode coupling of the incident laser light into two other waves. Of specific interest is when the two other waves are a scattered light wave and an electron plasma

wave. This process can best be described by looking at the motion of electrons in a plasma with an external electromagnetic field, and at the feedback loop leading to instability.

## 2. Plasma Oscillations and Waves

When an electron is displaced from a uniform background of ions, electric fields will be built up in such a direction as to restore the neutrality of the plasma by pulling the electrons back to their original positions [Ref.4]. The electrons will oscillate about an equilibrium position, at a characteristic frequency, the electron plasma frequency. (The ions are too massive and cannot respond, and are considered as a fixed background.) These plasma oscillations are electrostatic waves, which propagate through the plasma. Now let us consider how plasma waves can be driven unstable by an electromagnetic wave (in our case a laser). The instability cycle is described in Figure 2.

- (1) If we consider a uniform plasma, any small perturbations initially due to thermal noise can cause a small charge density fluctuation. This is a plasma oscillation with a noise level density fluctuation  $\delta n$ .
- (2) There is a perturbed current produced,  $\delta J$  ( $J$  being current density), which is equal to  $-e\delta n v_{os}$  (where  $e$  is the electron charge,  $\delta n$  is the density fluctuation, and  $v_{os}$  is the electron oscillating velocity). This  $\delta J$  is proportional to  $E_L \delta n$  ( $E_L$  being the electric field of the laser), and drives a scattered light wave at the beat frequency.
- (3) The scattered light wave grows from noise as a perturbed wave with electric field amplitude  $\delta E$  (a light wave at an up shifted or downshifted frequency).

- (4) This field in turn beats with the laser electric field to generate a variation in the wave pressure, proportional to  $\underline{E}_L \bullet \delta \underline{E}$ , which can reinforce the density fluctuation that we started with. This feedback leads to an exponential growth of both the plasma wave ( $\delta n$ ) and the scattered light wave ( $\delta E$ ).

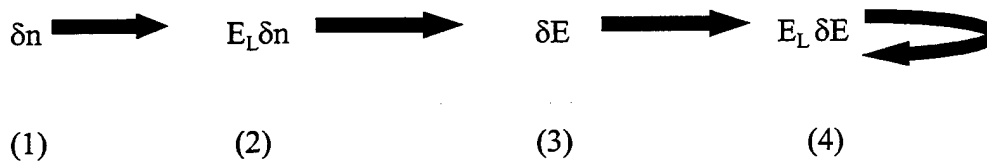


**Figure 2. Plasma instability feedback loop for Raman backscatter growing from noise.**

### 3. Coupled Oscillators and Frequency Matching

It is instructive to consider frequency and wave number matching for the instability. The laser at its frequency and wave number beats with the density fluctuation (at its frequency and wave number) driving scattered waves. The incident wave and scattered wave can then beat to reinforce the density fluctuation. The instability can grow if the beat frequency and wave number of the incident light wave and scattered light wave are at the characteristic frequency and wave number of the plasma wave.

The frequency matching and k matching equations are as follows:

$$\omega_o \rightarrow \omega_{sc} + \omega_{pe} \quad (1)$$

(an incident light wave with frequency  $\omega_o$  decays into a scattered light wave at a scattered frequency  $\omega_{sc}$  and a plasma wave at the plasma frequency  $\omega_{pe}$  including thermal correction)

The plasma frequency of a plasma is defined as:

$$\omega_{pe} = \sqrt{\frac{n e^2}{m \epsilon_o}} \quad (2)$$

where n is the density of the plasma, e is electron charge, m is electron mass. (It is useful to think of plasma density in terms of the critical density, the density at which light no longer propagates in a plasma, or when  $\omega_o = \omega_{pe}$ )

$$k_o = k_{sc} + k_{plasma} \quad (3)$$

(the spatial part of the waves must also match, where k is the wave number of the incident, scattered, and plasma wave respectively)

#### 4. Ponderomotive Force, the Physical Mechanism

The physical mechanism for the growth of the electron plasma wave is the ponderomotive force. The high radiation pressure of intense lasers creates a force that interacts with particles in a subtle way, called the ponderomotive force. A gradient in the electric field pressure, just like a gradient in the particle pressure, gives a force that pushes plasma from regions of high field intensity to regions of low field intensity. This ponderomotive force can be expressed as:

$$F_{nl} = -\frac{\omega_{pe}^2}{\omega^2} \frac{d}{dx} \left\langle \frac{\epsilon_0 E^2}{2} \right\rangle \quad (4)$$

where  $\langle \rangle$  denotes a time-average. If  $E = \underline{E}_L + \delta \underline{E}$ , there is a component of their force proportional to  $\underline{E}_L \bullet \delta \underline{E}$ , which drives a density fluctuation at the beat frequency.

When this beat frequency equals  $\omega_{ek}$  (the Bohm-Gross frequency), an electron plasma wave is driven up. The density fluctuation in turn couples with the incident laser light to give a larger  $\delta E$ , which beats with  $E_L$  to give a larger  $\delta n$  associated with the plasma wave. Due to this feedback, both an electron plasma wave and a scattered light wave exponentially grow, and causes the stimulated Raman instability.

#### 5. Dispersion Relation for a Light Wave in a Plasma

It is necessary to mention here briefly the dispersion relation for a light wave propagating in a plasma. The dispersion relation is obtained from Maxwell's equations for a light wave traveling through a system of charged particles. The relation will assist us in determining characteristics and magnitudes of values of the plasma.

The dispersion relation for a light wave in a plasma is defined as:

$$\omega_o^2 = k_o^2 c^2 + \omega_{pe}^2 \quad (5)$$

(The scattered light wave also obeys this dispersion relation.)

## 6. Dispersion Relation for Electron Plasma Waves

There is also the dispersion relation for the electron plasma waves. It is:

$$1 = \frac{\omega_{pe}^2}{k^2} \int_{-\infty}^{+\infty} \frac{\partial f / \partial v}{v - (\omega / k)} dv \quad (6)$$

(where  $k$  is the wave number of the plasma). Evaluating this integral shows that the frequency of the wave is the electron plasma frequency plus a thermal correction (the Bohm-Gross correction). In particular:

$$\omega_{ek}^2 = \omega_{pe}^2 (1 + 3k^2 \lambda_{De}^2) \quad (7)$$

where  $\lambda_{De}$  is the Debye length, the length at which local electrostatic potentials are shielded. It is evident that as  $k_{\text{plasma}}$  becomes larger, the phase velocity of the plasma wave is smaller (closer to the thermal velocity of the electron distribution), and the thermal correction becomes greater. There is also an imaginary component of the result of this integral, which physically describes a non-collisional damping term. The electrons near the phase velocity of the plasma wave can gain momentum at the expense of the wave, damping the wave. This effect is called Landau damping. The thermal correction is included in the calculations of frequency matching.

## 7. Types of Instabilities

There are three types of instabilities involving electron plasma waves when  $n$  is less than or equal to  $.25n_{cr}$ . ( $n_{cr}$  is the density at which light no longer can propagate through the plasma.) SRS occurs when  $n \leq .25n_{cr}$ , and the two plasmon decay for  $n$  approximately equal to  $.25 n_{cr}$ . An electron plasma wave can also decay into an electron plasma wave and an ion wave, which is called the Langmuir decay instability.

### Stimulated Raman scattering:

$$\omega_o \rightarrow \omega_{sc} + \omega_{pe} \quad (8)$$

Here the light wave decays into a scattered light wave and an electron plasma wave as just discussed.

### 2 Plasmon decay:

The frequency matching equation now gives:

$$\omega \rightarrow \omega_{ek} + \omega_{ek}, \text{ where } \omega_{ek}^2 = (\omega_{pe}^2 + 3k^2 v_{th}^2)$$

Since  $\omega_{ek} \approx \omega_{pe}$ , this instability occurs where  $n \approx 0.25n_{cr}$ .

In our case, the scattered light wave frequency is near  $2\omega_{pe}$ . Hence it can in principle decay into two electron plasma waves, producing more hot electrons. This additional hot electron generation is possible but may not be a large effect unless the scattered wave intensity becomes large and the plasma is rather uniform in density.

### **Stimulated Brillouin scattering:**

To completely understand the characteristic behavior of plasmas, the formation of ion waves and their effects must be included. Though ions cannot respond fast enough to the frequency of an electromagnetic wave, the light wave can decay into a scattered light wave and an ion acoustic wave, otherwise known as stimulated Brillouin scattering. The ion acoustic wave is at a frequency that the ions like to oscillate; thus ion motion needs to be included. Ion fluctuations will later be shown to have an effect on the growth of the forward SRS. SRS is seen at all densities up to the critical density.

### **8. Electron Heating Due to Growth of SRS and Two Plasmon Decay**

Electrons in the plasma are heated by electron plasma waves associated with either SRS or with the two-plasmon decay instability. As the SRS instability grows, a plasma wave with a high phase velocity,  $v_{\text{phase}}$ , grows. Electrons that are moving slower than the electron plasma wave can get caught in the potential of the wave. As they fall in this potential they are accelerated to velocities of order of the phase velocity. This leads to the creation of a high-energy tail on the electron distribution function. An effective temperature of these heated electrons is of order  $mv_{\text{phase}}^2/2$ .

### **9. Instability Cycle for Forward SRS using Seed Beam**

The forward SRS can be exploited if we take  $3\omega$  light and "seed" it with a light wave at the exact frequency of the scattered light wave. The field then grows not just from noise, but starts from the level of the seed beam. The instability cycle now looks like this:

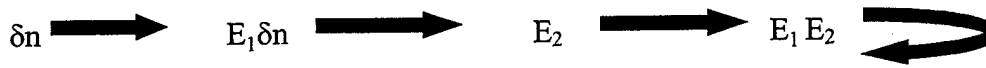


**Figure 3. Forward Raman Scattering Instability Cycle with Seed Beam.**

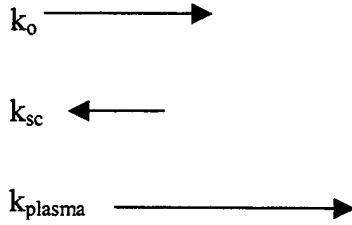
This instability can become the dominant instability. The ponderomotive force now contains the seed component, which biases the scattering to occur in this direction. This instability produces an electron plasma wave of much greater phase velocity. Also, the angle between the two beams can be varied, which can vary the value of the phase velocity. This can be best explained by looking at the wave number matching equations for the forward and backscatter Raman instabilities.

### **10. Hot Electron Generation through Seeding of Forward SRS**

To develop x-ray sources, one may aim to efficiently generate very energetic electrons. This can be done by seeding Raman scattering in the forward direction, either directly forward or in general at some angle  $\theta$ . ( $\theta=0$  corresponds to direct forward scattering.) It is instructive to consider wave number and frequency matching for backscatter, for direct forward scatter, and for forward scatter at an angle.

First consider the  $k$  matching for backscatter, where  $\underline{k}_0 = -\underline{k}_{sc} + \underline{k}_{plasma}$ , or  $\underline{k}_{plasma} = \underline{k}_0 + \underline{k}_{sc}$ :

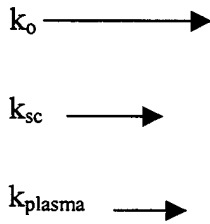
In vector form:



The k matching equations are shown below for forward scatter:

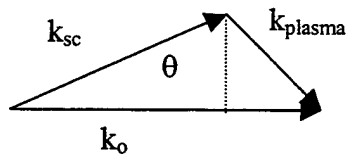
$$k_o = k_{sc} + k_{plasma} \text{ or } k_{plasma} = k_o - k_{sc}:$$

In vector form:



So in the forward case  $k_{plasma}$  is smaller, giving us a greater phase velocity of the plasma wave.

In fact, the phase velocity of the plasma wave can be varied by changing the angle between the incident and scattered light ( $\theta$ ). The wave number of the plasma wave is obtained by vector addition:



$$k_{\perp} = k_{sc} \sin \theta \quad (9)$$

$$k_{parallel} = k_o - k_{sc} \cos \theta \quad (10)$$

$$k_{plasma} = \sqrt{k_{sc}^2 \sin^2 \theta + (k_o - k_{sc} \cos \theta)^2} \quad (11)$$

$k_{plasma}$  is then found by taking the magnitude of the perpendicular and parallel components of  $k_{plasma}$ .

Consider a specific case where  $\omega_o = 3\omega_{pe}$ . By using the frequency and k-matching equations, and the dispersion relation for a light wave in a plasma, the value of  $k_{\text{plasma}}$  can be derived. First, since  $\frac{\omega_{pe}}{\omega_o} = \frac{1}{3}$ , frequency matching gives  $\frac{\omega_{sc}}{\omega_o} = \frac{2}{3}$ , where for this illustration we neglect the thermal correction. Using the dispersion relation for light waves,  $\frac{k_o c}{\omega_o} = 0.94$  and  $\frac{k_{sc} c}{\omega_o} = 0.58$ .

So, by k matching ( $k_o = k_{sc} + k_{\text{plasma}}$ ) for backscatter  $k_{\text{plasma}} c / \omega_o = 1.52$ . The phase velocity of a wave is defined as  $\frac{\omega_{pe}}{k_p} = v_{\text{phase}}$ , so the phase velocity would be

$$\omega_{pe} / \left( 1.52 \frac{\omega_o}{c} \right) = (c/3) / 1.52 = 0.22c.$$

In contrast, by "seeding" the  $3\omega$  with  $2\omega$ , our frequency matching gives us a frequency of  $\omega_{pe}$  in the forward direction. By doing k matching in the forward direction, it is shown that the  $k_{\text{plasma}}$  only makes up the difference of the incident k and  $k_{\text{scattered}}$ , giving a  $k_{\text{plasma}} c / \omega_o = 0.36$  and a  $v_{\text{phase}} = 0.93c$ . Further, if the scattered wave is at an angle of 30 degrees,  $k_{\text{plasma}}$  is at a larger value of  $k_{\text{plasma}} = 0.36$  and  $v_{\text{phase}} = 0.63c$ .

Just from this calculation, we can estimate the electron energy from forward scattering using  $\frac{1}{2} m v_{\text{phase}}^2$ . If we say that the rest mass energy ( $E = mc^2$ ) of an electron is 511 keV, then  $\frac{1}{2} (511 \text{ keV}) (.93)^2 = 220 \text{ keV}$ , and at an angle, i.e. 30 degrees,  $E = 173 \text{ keV}$ . (For convenience, we shall ignore in the estimate the relativistic effects of electrons moving close to the speed of light. Relativistic effects are included in our simulations.)

By sending along a light wave at  $2\omega_o/3$ , (i.e. 0.53 micron light) forward scattering can be seeded and a high phase velocity plasma wave is generated. More generally, this 0.53  $\mu\text{m}$  light will be sent along at some angle, generating a lower phase velocity wave. Since we will use 0.35 and 0.53  $\mu\text{m}$  light, the plasma density will be  $n_{cr}/9$  for the 0.35 $\mu\text{m}$  light (actually a little less when the Bohm-Gross corrections are included.) Hence the plasma density will be approximately  $10^{21}/\text{cm}^3$ .

## **11. Summarization of Growth Rates for Backscatter and Seeded Forward**

### **Scatter**

Both forward scatter and backscatter occur with the instabilities growing from noise with just one beam at 0.35  $\mu\text{m}$ . The backscatter SRS is dominant, however, as the growth rate depends on the magnitude of  $k_{\text{plasma}}$ , and therefore backscatter grows at a faster rate. When using a seed beam to seed the forward instability, the growth rate starts at a much higher level than noise, and can become the dominant instability. We note that there have been some recent experiments [Ref. 5] in which Stimulated Raman backscatter was seeded.

## **B. COMPUTER SIMULATION OF ELECTROMAGNETIC WAVE IN A PLASMA**

### **1. Theory of Computer Simulation for Plasmas**

It is quite useful to use computer simulations to model laser-plasma interactions, since non-linear effects become important, and the energy distribution of the particles can be strongly modified. Analysis then becomes very difficult increasing the value of computer simulation. With the increasing demand for laser experiments and the few resources available, it is appropriate to first test theoretical predictions through simulation.

There are some modern computer codes available for the simulation of plasma behavior [Ref. 6,7]. These types of codes are called relativistic, electromagnetic particle-in-cell codes. They use two principles to imitate the behavior of a plasma: They solve Maxwell's equations to calculate the fields due to the charge and current density of the particles. They solve equations of motion using the Lorentz force.

The charge and current density due to the particles are assigned to a grid using an area-weighting (or linear-interpolation) scheme. The electric and magnetic fields on this grid are then determined by finite-differencing Maxwell's equations. Finally, the Lorentz force is determined by interpolating these fields to the particle positions. The positions and velocities are updated using a leap-frog scheme. More details of the PIC code development can be found in reference [6].

## 2. Setting the Conditions for the Computer Simulation using Turbowave

We use here a simulation code called Turbowave written by Dan Gordon [Ref. 6]. It is convenient to work in terms of dimensionless values when conducting computer simulations. For example, the frequency of the incident light wave is normalized to  $\omega_{pe}$ . For example, in a simple case, we can send in a light wave with normalized frequency at  $\omega_o/\omega_{pe}=3$ , that is,  $\omega_o=3\omega_{pe}$ . The intensity of the wave is also input as a dimensionless quantity  $a=eE_o/m\omega_o c$ , where  $E_o$  is the electric field of the light wave,  $\omega_o$  the frequency, and  $c$  the velocity of light. It can be shown that  $a^2=\frac{I\lambda_\mu^2}{1.35\times 10^{18}}$ , where  $I$  is the laser intensity in Watts/cm<sup>2</sup> and  $\lambda_\mu$  the vacuum wavelength in microns.

The specific input parameters for these simulations are then as follows:

$a$ : 0.1 and 0.03 (for  $\omega_1=3\omega_{pe}$  and  $\omega_2=2\omega_{pe}$ )

*Mass ratio (adjusts ion movement):*  $m_{ion} \sim 100-1000m_e$

*Initial electron thermal velocity:*  $v_{th}=0.07c$ ;  $v_{th}/c=0.07$  ( $\sim 2.5$  keV)

*Ion temperature:* 0.625 keV

$Ti/Te=1/4$ : ( $Ti$  and  $Te$  are temperatures of ions and electrons, respectively) specifies ion Landau damping of the ion waves. By varying ion temperature, the ion wave damping can be varied.

*cell size:*  $.1 c/\omega_{pe}$  (which is larger than Debye length of  $0.07 c/\omega_{pe}$ )

*System size ( in units of  $c/\omega_{pe}$ ):* For example, a system size of 512 by 128 corresponds to  $51.2 c/\omega_{pe}$  by  $12.8 c/\omega_{pe}$ .

*Particles/cell:* any number\*

\* Simulation limited by: (100 x total #of particles) must be less than RAM available in computer system

To simply illustrate the effects, we typically use  $a=.1$  for the 0.35 micron light.

This corresponds to an intensity of  $1.1 \times 10^{17} \text{ W/cm}^2$ .

THIS PAGE INTENTIONALLY LEFT BLANK

### III. RESULTS AND ANALYSIS

#### A. SIMULATIONS OF $3\omega$ (BACKSCATTER) AND $3\omega$ AND $2\omega$ (SEEDED FORWARD SCATTER)

##### 1. Introduction

To demonstrate the effect of the seeding of forward scatter, it is first instructive to look at the case of using just  $0.35\text{ }\mu\text{m}$  light alone and see how much heating is caused by primarily Raman backscatter. Then, the second case adds a seed beam of  $0.53\text{ }\mu\text{m}$  to induce the Raman forward scatter instability, demonstrating a significant increase in the amount of electron heating. Then, by introducing an angle between beams, (in the case shown the angle is 30 degrees) it can be demonstrated that the increased  $k_{\text{plasma}}$  gives a smaller phase velocity of the plasma wave, thereby lowering the electron temperature. In all of these cases the ions are treated as fixed. The final case introduces moving ions, which introduces large density fluctuations. For convenience, the mass ratio has been reduced to 100, which separates the electron and ion timescales while allowing quicker simulations.

The first two simulations are one-dimensional. Quantities are allowed to vary only in the x-direction, which is the direction in which the light waves propagate. In the two-dimensional simulations, variations in both the x and y directions are allowed. In the cases discussed here, the electric vector of the light wave is in the z-direction. Future simulations will explore the case with this electric vector in the y-direction, which will allow the two-plasmon decay instability to be included.

## 2. Case 1: Raman Backscatter

In our first case, only 1 beam of frequency  $3\omega_{pe}$  is injected into the plasma at an intensity of  $a=0.1$ . Figure 4 shows the incident light wave as well as the scattered light wave at  $2\omega_{pe}$ . Figure 5 shows the effect of the ponderomotive force of the incident light wave and the scattered light wave, producing an electron plasma wave, oscillating at the plasma frequency. (Figures 4 and 5 are plotted as the oscillating velocity vs.  $x$ ). Figure 6 shows the momentum of the electrons within the plasma wave versus the length of the plasma. Electrons are heated as they are accelerated to the phase velocity of the electron plasma wave. The energy plot shows the incident light wave, the left pointing flux (incident and scattered at the left boundary), the field energy in the system, the kinetic energy of the particles in the system, the energy of the particles lost out of the system, and the right poynting flux (light wave leaving the system.) The distribution plot shows the heated electron tail of the electron distribution, with the distribution on a log scale (y-axis) and energy to 1 Mev (x-axis). From this, the temperature of the electron tail can be obtained by assuming a distribution function that goes as  $\exp [-E/k_B T]$ . By taking a multiple of log drops for the distribution and for what range of energy the drop occurs, we can determine an approximate temperature for the electrons by solving for  $T=E/ (2.3 * \text{\#of drops})$ . (This range is depicted as a straight line through the distribution tail.) For the first case about 7% of the laser is absorbed into hot electrons, with an electron temperature of  $\sim 26$  keV. These values do show that there is some instability growth, and heating of electrons in this strongly driven example.

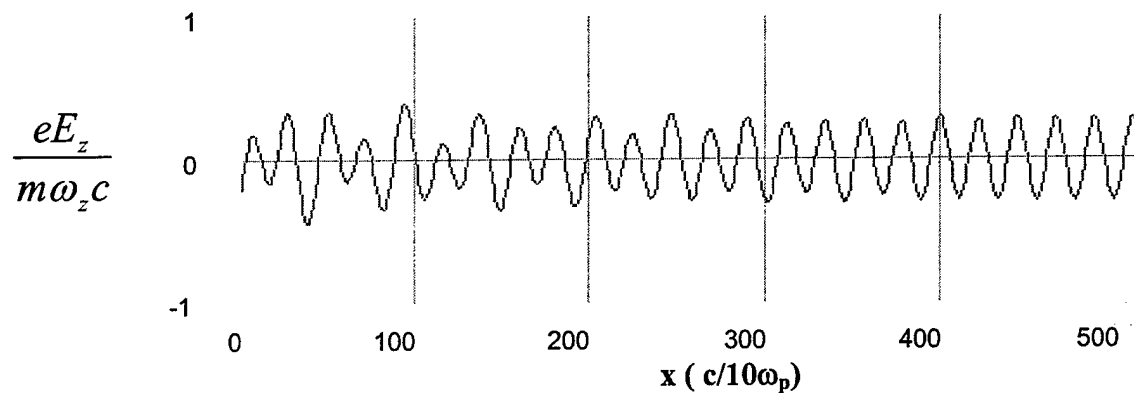


Figure 4. Electric Field in z-direction.

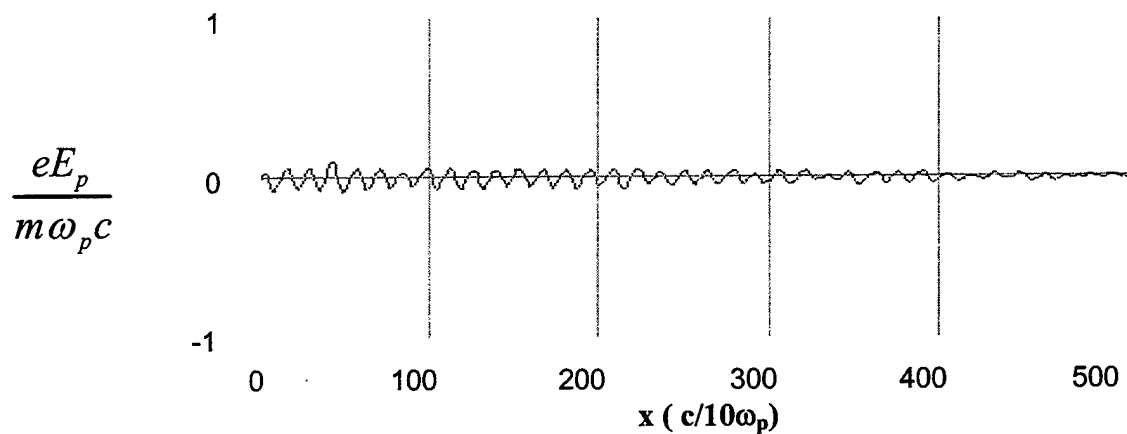


Figure 5. Electron Plasma Wave Electric Field in x-direction.

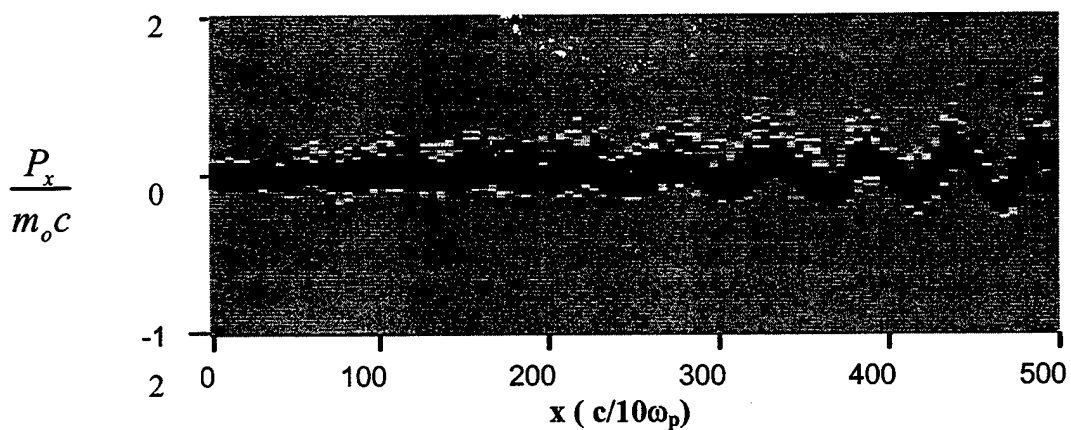
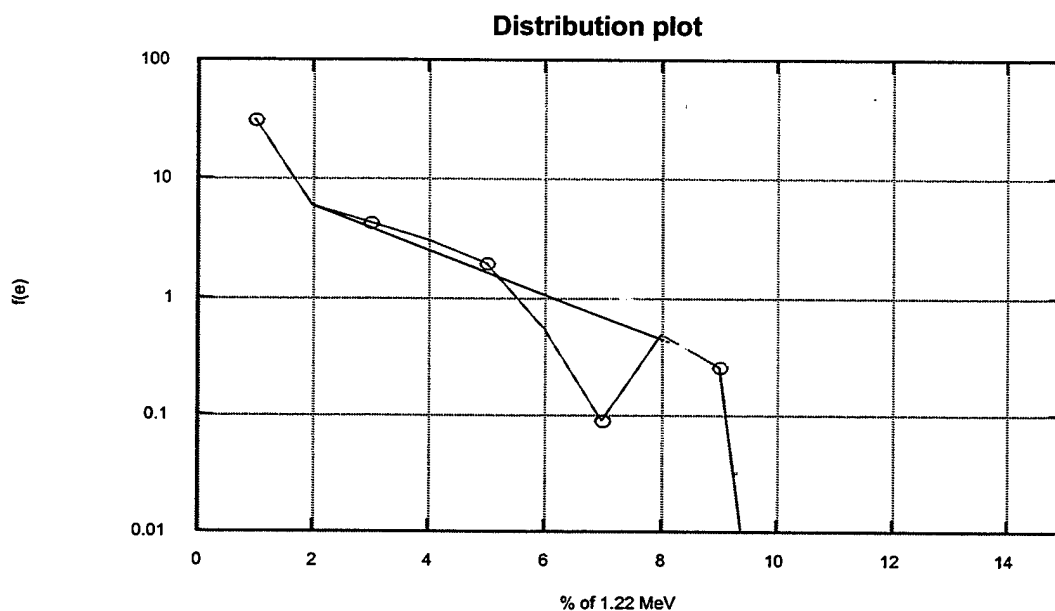
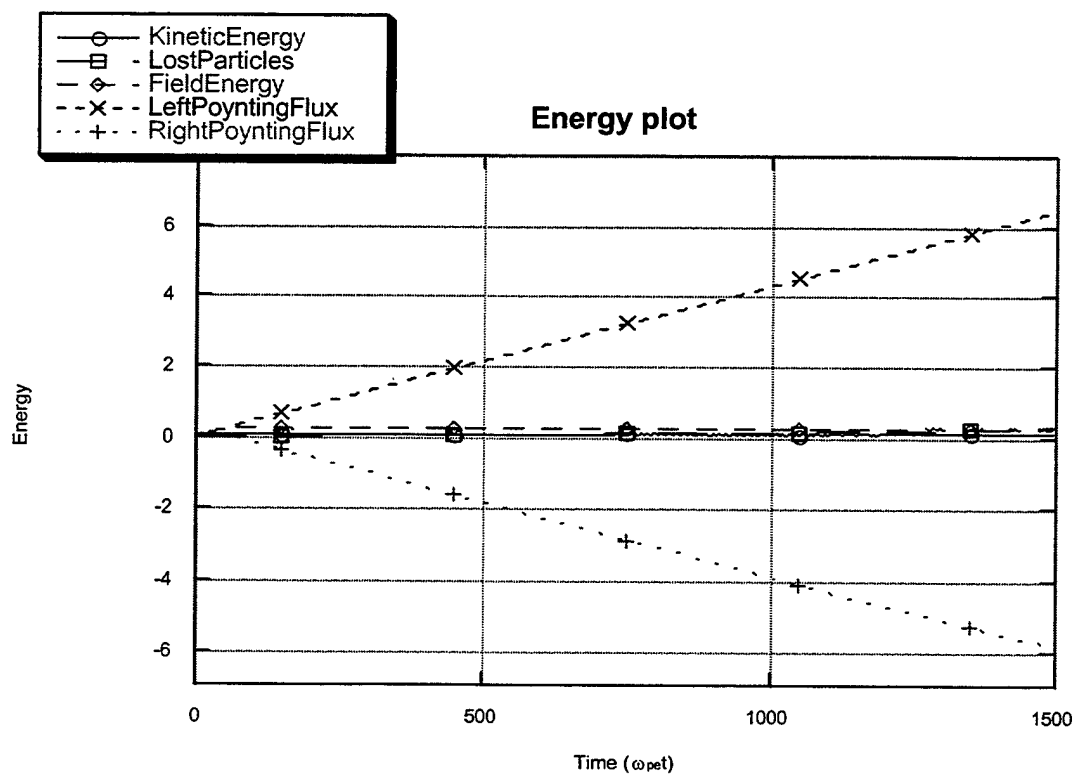


Figure 6. Momentum of Electrons in Plasma Wave.



**Figures 7 and 8. Energy and Electron Distribution Plot for SRS Backscatter**  
 (straight line on distribution plot depicts energy range to determine temperature).

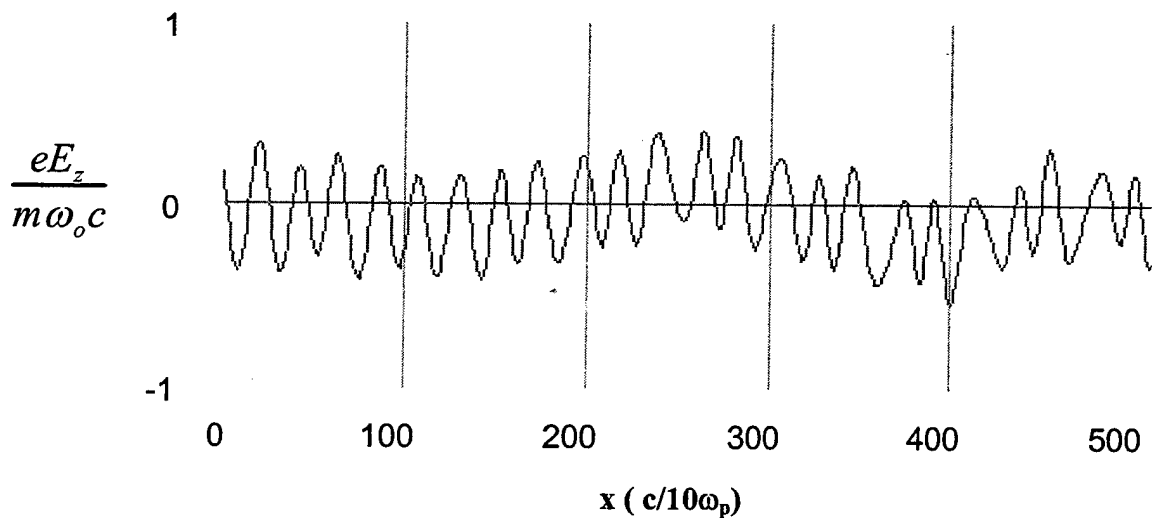


Figure 9. Electric field in z-direction.

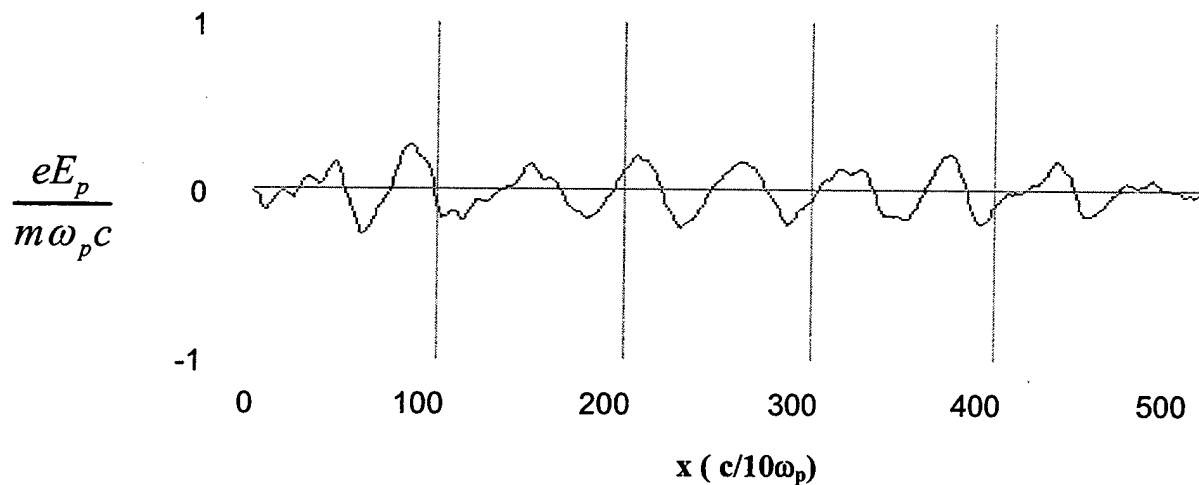


Figure 10. Electron plasma wave electric field in x-direction.

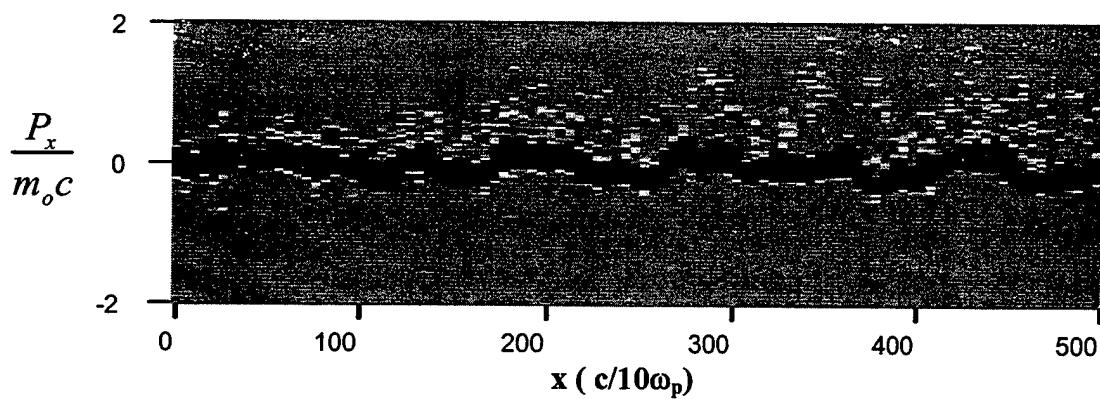
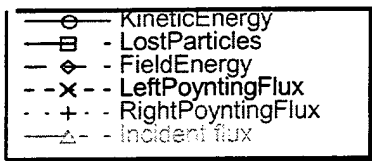


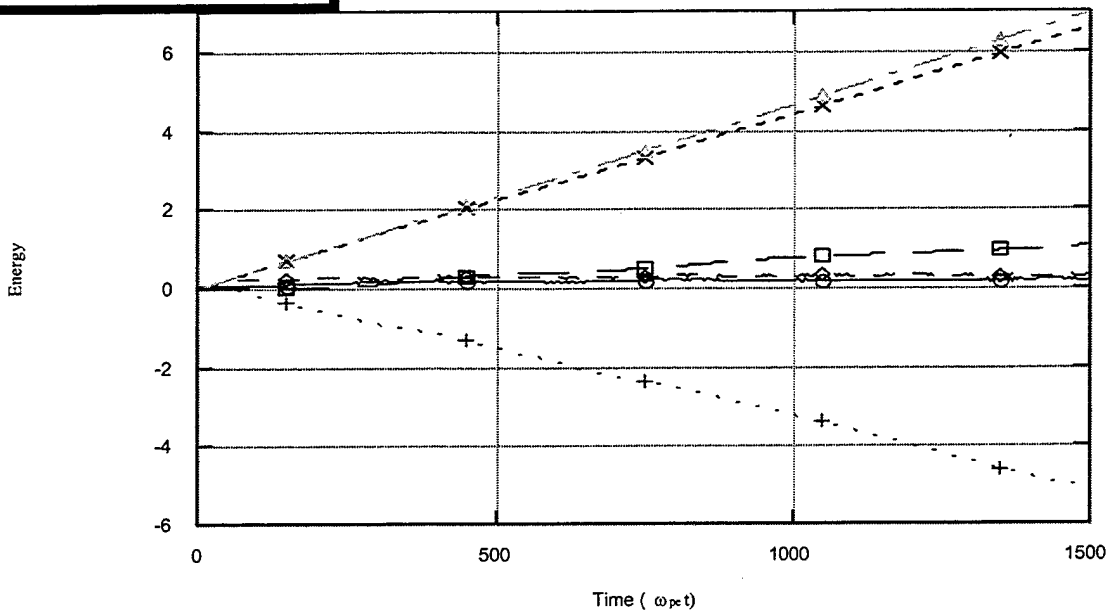
Figure 11. Momentum of electrons in plasma wave.

## 2. Case 2: Seeded Forward Scatter

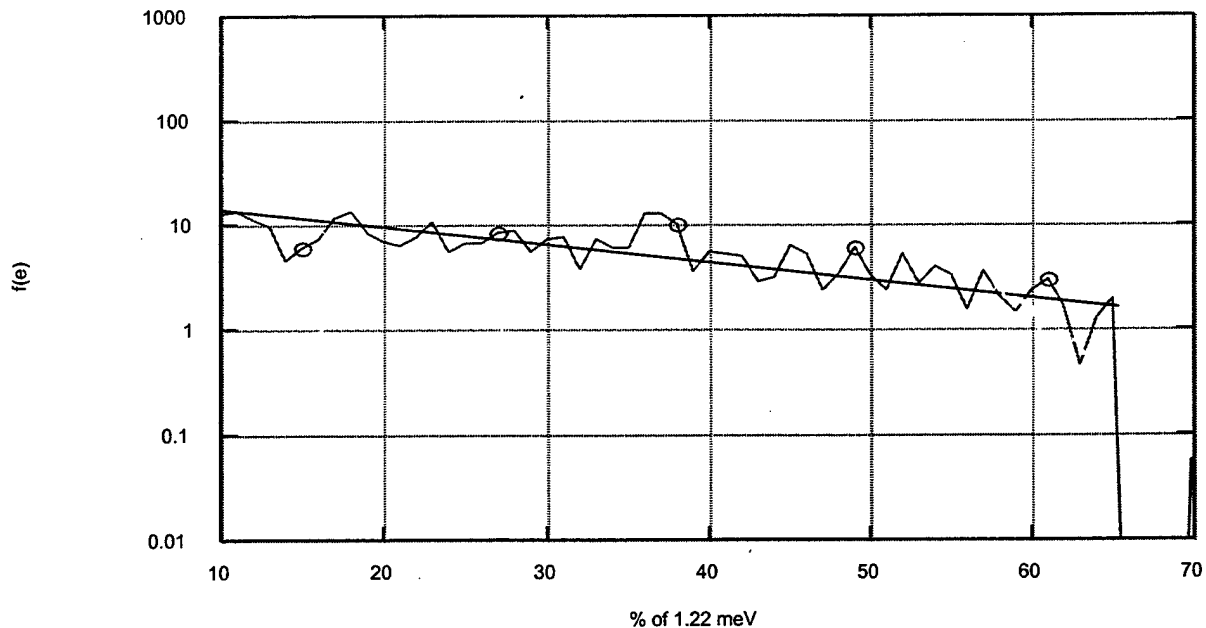
In this case, 1 beam of frequency  $3\omega_{pe}$  is injected at  $a=0.1$  into the plasma with a parallel seed beam at  $2\omega_{pe}$  at  $a=0.03$ . The growth of the instability is now much more significant, with an electron plasma wave at a much higher phase velocity. Figure 9 shows the electric field of the incident light wave, scattered light wave, and the decay of the scattered light wave can be seen. The electron plasma wave electric field is shown in Figure 10, and there is more heating of the electrons than in Case 1, as shown in the Figure 11, the electron momentum plot. The absorption of the light wave into hot electrons is about 20 percent, with an electron temperature of about 240 keV. Compared to Case 1, it is evident that the seeding of the forward case more efficiently heats electrons and to higher temperatures.



Energy plot



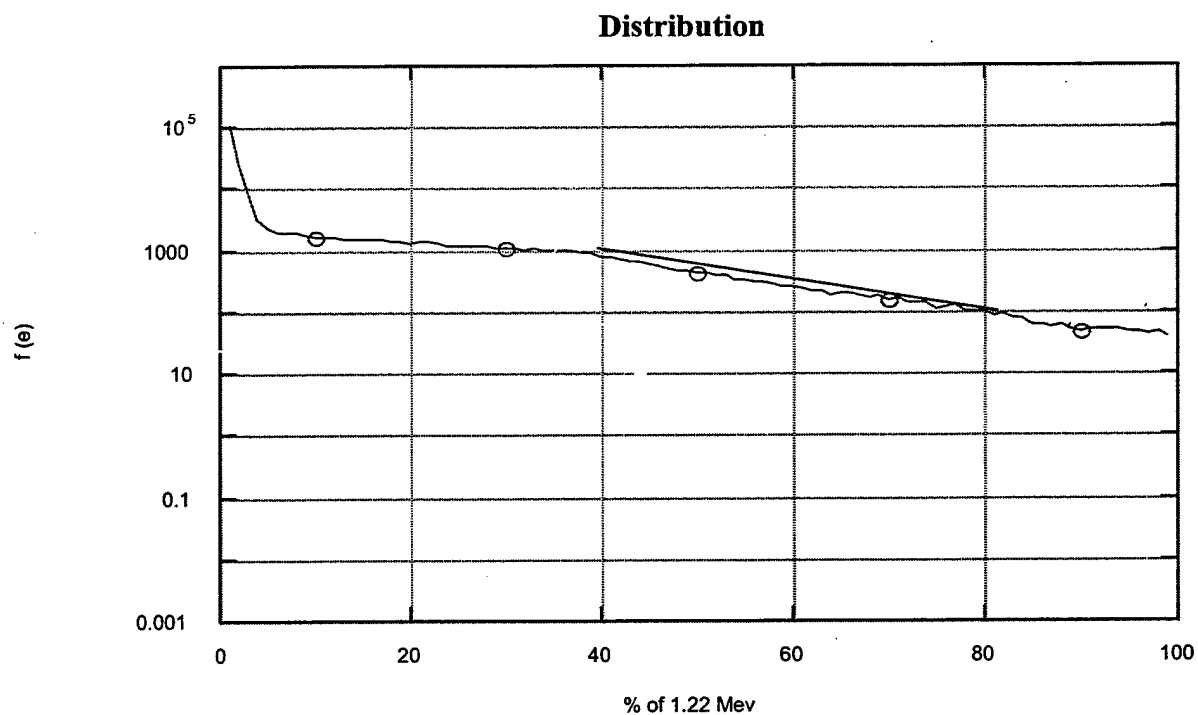
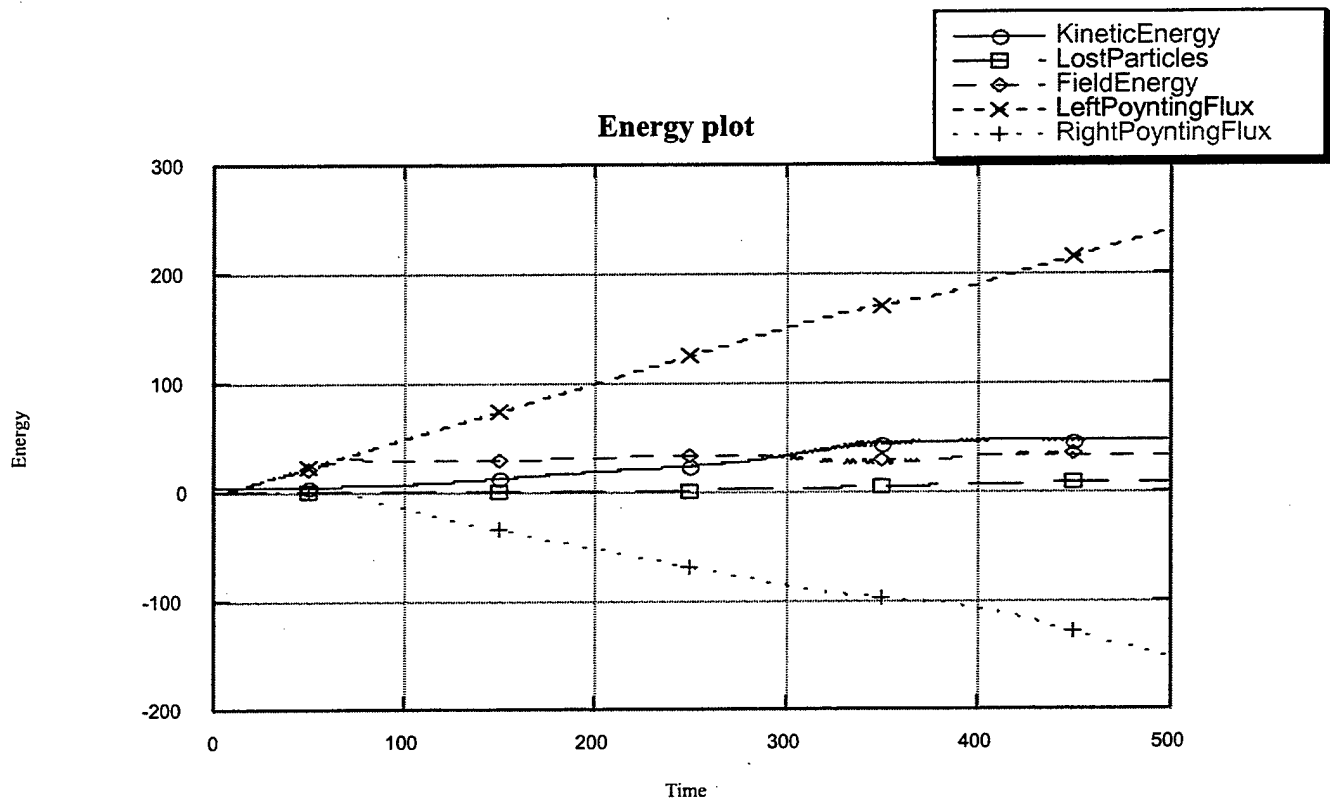
Distribution plot



**Figures 12 and 13. Energy and Distribution Plots for Seeded Forward SRS.**  
By "seeding" forward SRS, high absorption into hot electrons occurs (straight line on distribution plot depicts energy range to determine temperature).

### 3. Case 3: $3\omega$ and $2\omega$ at a 30 Degree Angle

To demonstrate the effect of crossing the beams at some angle, an example of 30 degrees is used here. The corresponding absorption remains relatively the same, but the electron temperature is reduced to  $\sim 173$  keV. This reduction in temperature is expected; as  $k_{\text{plasma}}$  increases,  $v_{\text{phase}}$  of the electron plasma wave decreases, and therefore heating of electrons to a lower temperature.



**Figures 14 and 15. Energy and Electron Distribution for Seeded Forward SRS at a 30-Degree Angle Between Beams (straight line on distribution plot depicts energy range to determine temperature).**

#### 4. Effect of Ion Density Fluctuations

To see the role moving ions play in the growth of the instability, the mass ratio was decreased and the temperature was adjusted to correspond to a fairly damped ion wave case ( $T_i/T_e=.25$ ). Large ion density fluctuations develop [Fig. 16], which disrupts the growth of forward SRS. This effect on the forward SRS depends on the value of  $k_{\text{plasma}}$ , as the growth rate depends on  $k_{\text{plasma}}$ . In the parallel beam case,  $k_{\text{plasma}}$  is small, so ion density fluctuations have a large effect on the instability. However, as the angle increases between the beams, and thus  $k_{\text{plasma}}$ , the growth rate is correspondingly higher, and so the ion fluctuations are less of a factor. Figures 17 and 18 show the effect of ion fluctuations in the seeded forward SRS simulations.

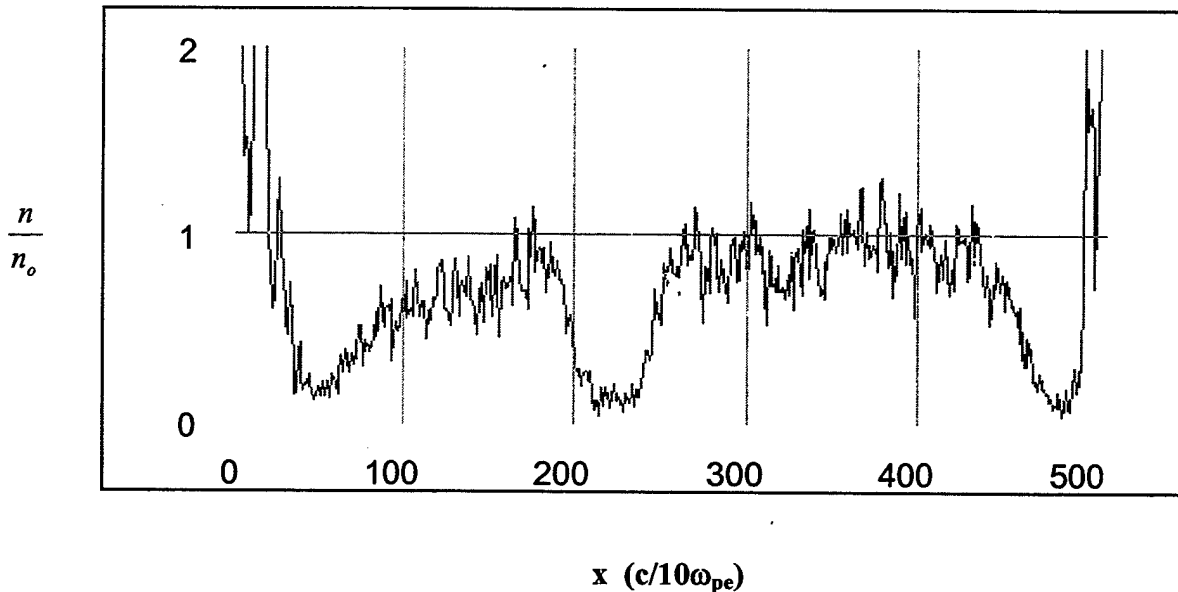
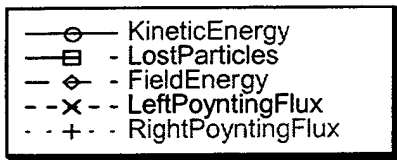
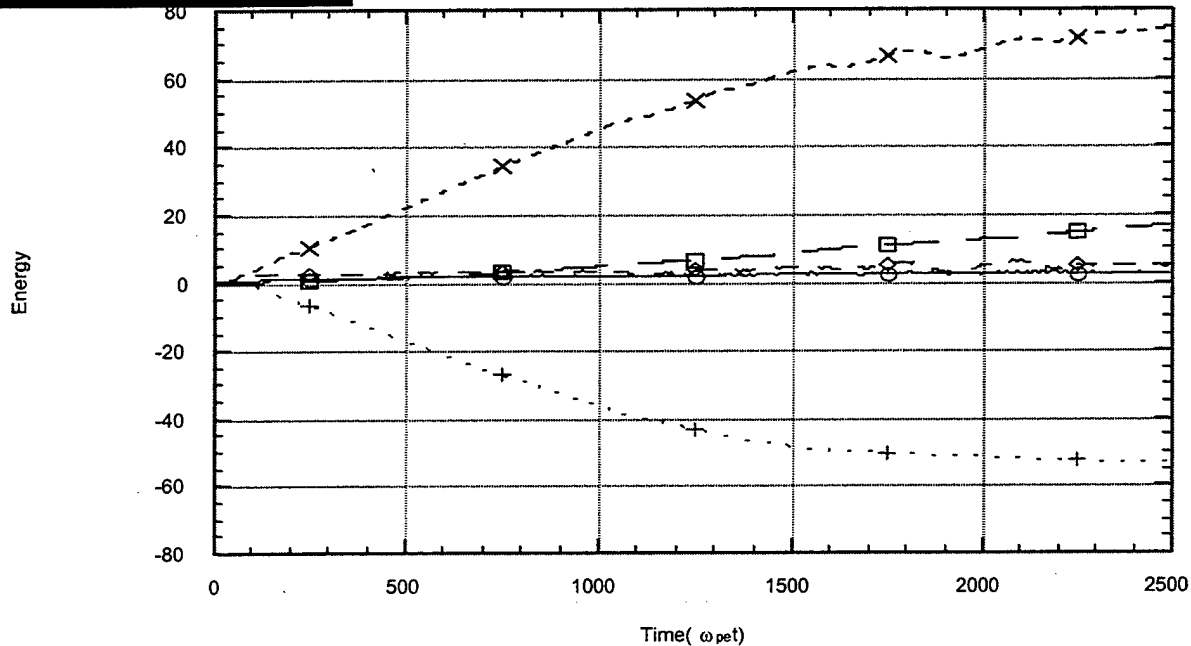


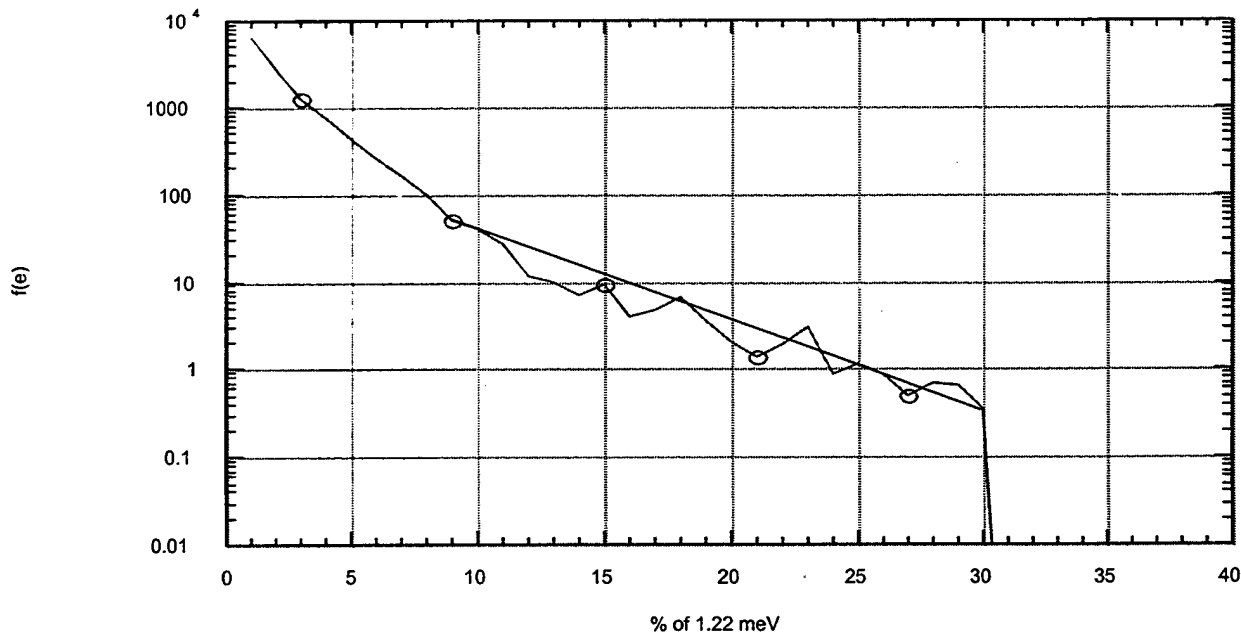
Figure 16. Ion plot for  $3\omega$  and  $2\omega$



**Energy plot**



**Distribution plot**



**Figures 17 and 18. Energy and Electron Distribution plots with Ti/Te=0.25. Note the lower electron temperature (compared to Case1) as a result of ion fluctuations (straight line on distribution plot depicts energy range to determine temperature).**

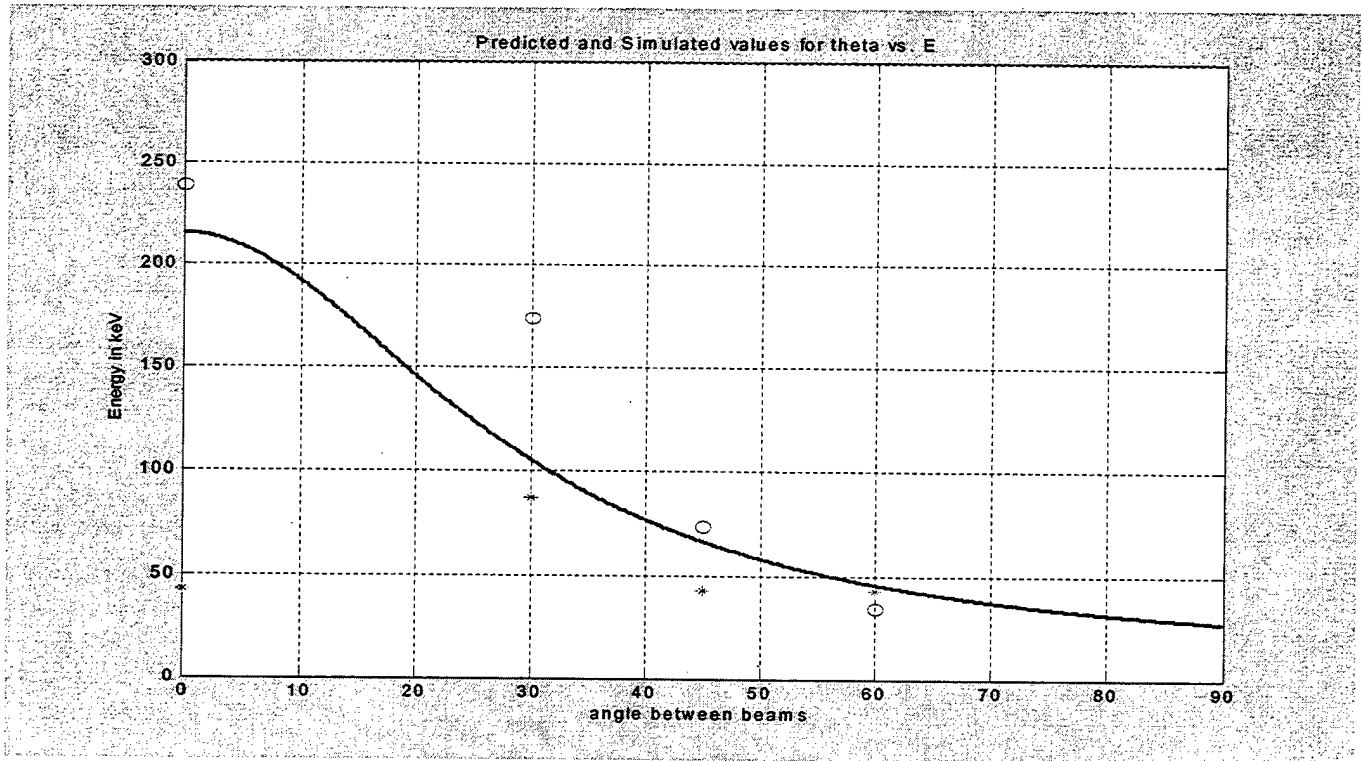


**Figure 19. Estimated and Simulated values of the hot electron temperature vs. angle. (Simulations were done in 2D, with  $\omega_1=3\omega_{pe}$ ,  $a=.1$ ;  $\omega_2=2\omega_{pe}$ ,  $a=0.03$ )**

Solid line: Theoretical estimate  
 o : Simulation values, ions fixed  
 \*: Simulation values, fairly damped ions

## B. DATA ANALYSIS

### 1. Analysis of Estimated and Simulated Values

We can estimate the temperature of electrons using  $mv_{\text{phase}}^2/2$  (solid curve) as the angle between beams increases [Fig. 19]. (We note that we have not attempted to include relativistic effects in the crude estimate.) The circles correspond to simulated data at angles of 0, 30, 45 and 60 degrees with fixed ions. The asterisk plot represents the same simulations with moving ions and fairly damped ion waves ( $T_i/T_e = .25$ ). At  $\theta=0$ , (direct forward scatter), ion fluctuations greatly reduce the heated energy. As the angle

increases,  $k_{\text{plasma}}$  increases, as does the instability growth rate. The ion density fluctuations then have less of an effect. Table 1 summarizes the estimated and simulated values for different angles with and without ions. As one can see, the increase in angle between beams decreases the  $T_{\text{hot}}$  of the electrons. When one includes the movement of ions (the  $T_{\text{hot}}$  w/ ions column), the large density fluctuations disrupt the instability and there is a significant drop in the  $T_{\text{hot}}$ . Since the instability growth rate is small in the parallel case, this is where one can see a dramatic effect on  $T_{\text{hot}}$ . As the angle increases,  $k_{\text{plasma}}$  increases, being proportional to the growth rate, and thus the ion fluctuations have less of an effect on the instability. Absorption (%abs) into hot electrons stays fairly constant throughout.

| $\theta$ | $\frac{m v^2}{2}$ | $T_{\text{hot}}$<br>(no<br>ions) | % a b s | $T_{\text{hot}}$<br>(w /<br>ions). | % a b s |
|----------|-------------------|----------------------------------|---------|------------------------------------|---------|
| 0        | 2 2 0             | 2 4 0                            | 2 0     | 4 3                                | 2 0     |
| 3 0      | 1 1 0             | 1 7 3                            | 2 0     | 8 7                                | 1 1     |
| 4 5      | 6 5               | 7 0                              | 1 0     | 4 4                                | 1 0     |
| 6 0      | 4 8               | 4 0                              | 1 4     | 3 3                                | 1 5     |

**Table 1. Summary of Estimated and Simulated Values of  $T_{\text{hot}}$  and percent of energy absorption (%abs) into hot electrons with fixed ions and moving ions.**

( $2D$ ,  $\omega_1=3\omega_{pe}$ ,  $a=0.1$  ;  $\omega_2=2\omega_{pe}$ ,  $a=0.03$ )

## 2. Absorption Peak for Density Variation in Plasmas

The .53  $\mu\text{m}$  light will seed Raman forward scatter of 0.35  $\mu\text{m}$  light when the frequency difference nearly matches the Bohm-Gross frequency in the plasma. The resonant behavior is demonstrated by varying the plasma density in a number of 1D simulations. This was done by changing the ratio of the plasma frequency (which is density dependent) to the frequency of the 0.35  $\mu\text{m}$  light from 1/2.9 to 1/3.16 (circular data points on graph. A best curve fit is applied to the data points). Notice in the Figure 20 below the expected resonance in the hot electron generation. The resonance is strong over a range corresponding to a density variation of about 5% ( $\Delta n/n=5\%$ ).

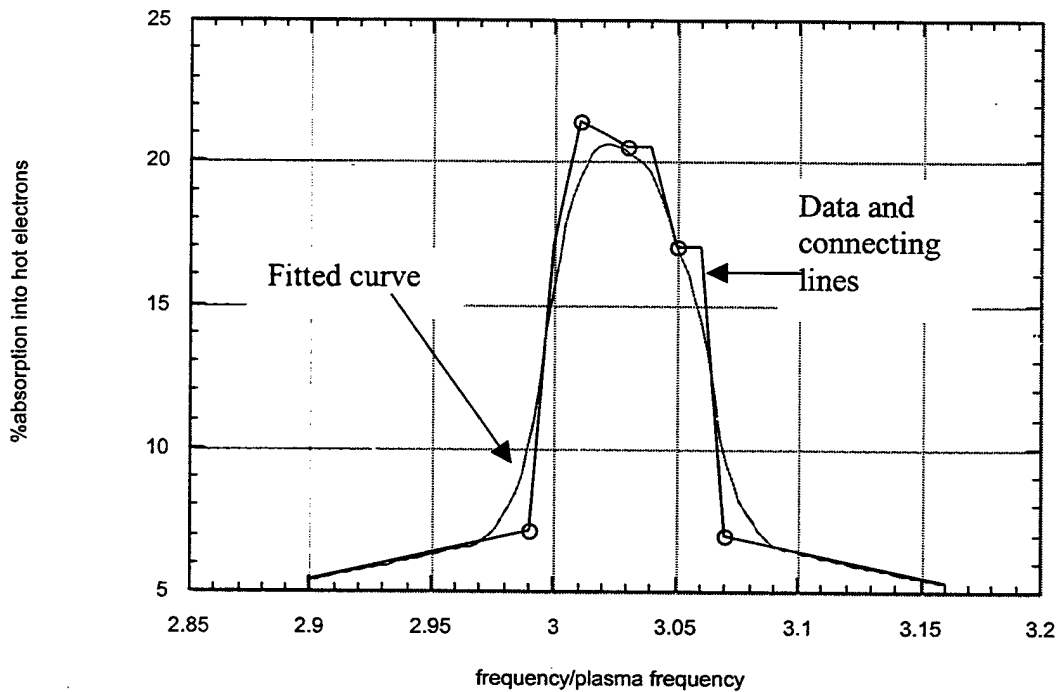


**Figure 20. Resonance Absorption Peak for 0.35 micron Light.**

#### IV. CONCLUSIONS

The Stimulated Raman scattering instability grows in both the forward and backward directions. When the instability grows from noise, the dominant instability is the backscatter. However, it has been shown through simulations that by seeding the forward scatter with a beam at the frequency of the scattered light wave, the instability is intensified and grows to significant levels. Electron plasma waves of high phase velocity grow, accelerating electrons to very high temperatures. Angling the beams varies the temperatures of the electrons, a method to control the heated electron energies and correspondingly the energy range for the desired output of x-ray flux. It was found that by introducing ion motion in the plasma, large ion density fluctuations developed, weakening the forward scattered instability. As the angle between beams is increased, however, the ion fluctuations have a smaller effect in the instability growth.

Because one cannot assume uniform densities because of gradients within the plasma during laser-plasma interactions, it was interesting to determine over what range of densities the seeded instability would still give significant absorption. It was found that there could be approximately 2.5% variation of density on either side of the resonant density and still get significant absorption into hot electrons to occur.

THIS PAGE INTENTIONALLY LEFT BLANK

## LIST OF REFERENCES

1. Kruer, William L., *Interaction of Plasmas with intense lasers*, Physics of Plasmas, Volume 7, Number 6, June 2000, and many references therein.
2. Kruer, William L., *Strongly driven laser-plasma coupling*, IOP Publishing, Ltd., UK, 1998.
3. R.K. Kirkwood, private communication, 2001.
4. Chen, Francis F., *Introduction to Plasma Physics and Controlled Fusion, Vol I.*, Second Edition, (Plenum Press), New York, NY, 1984.
5. R.K. Kirkwood, D.S. Montgomery, B.B. Afeyan, J.D. Moody, B.J. MacGowan, C. Joshi, K.B. Wharton, S.H. Glenzer, E.A. Williams, P.E. Young, W.L. Kruer, K.G. Estabrook, and R.L. Berger. *Observation of the nonlinear saturation of Langmuir waves driven by ponderomotive force in a large-scale plasma*, Phys. Rev. Lett. 83,2965 (1999).
6. D.F. Gordon et al., IEEE Trans. Plasma Sci. 28, 1224 (2000).
7. Startsev, Edward A., *Ponderomotive Particle Acceleration in a Plasma*, Laboratory Report 320, Laboratory for Laser Energetics, University of Rochester, December 2000.

THIS PAGE INTENTIONALLY LEFT BLANK

## INITIAL DISTRIBUTION LIST

1. Defense Technical Information Center.....2  
8725 John J. Kingman Road, Suite 0944  
Ft. Belvoir, VA 22060-6218
  
2. Dudley Knox Library.....2  
Naval Postgraduate School  
411 Dyer Road  
Monterey, CA 93943-5101
  
3. Engineering and Technology Curricular Office, Code 34.....1  
Naval Postgraduate School  
Monterey, CA 93943
  
4. Professor William L. Kruer, Code PH/Kw.....1  
Naval Postgraduate School  
Monterey, CA 93943-5002
  
5. Professor William B. Colson, Code PH/Cw.....1  
Naval Postgraduate School  
Monterey, CA 93943-5002
  
6. DTRA.....1  
8725 John J. Kingman Road  
MSC 6201  
Fort Belvoir, Va. 22060-6201
  
7. Michael A. Ortelli.....1  
P.O. Box 656  
Pinehurst, NC 28370
  
8. Physics Department .....2  
Naval Postgraduate School  
833 Dyer Road  
Monterey, CA 93943-5002